Peter Bächler*
Jörg Meyer
Achim Dittler

Operating Behavior of Pulse Jet-Cleaned Filters Regarding Energy Demand and Particle Emissions – Part 1: Experimental Parameter Study

Filter operation of a pilot-scale baghouse filter was evaluated under energy and particle emission criteria. Evaluation of the required total power for filter operation takes into account the fan power as well as the consumption of pressurized air. Filter face velocity, raw-gas concentration, and tank pressure for regeneration were varied for several cycle time settings to identify the minimum power. Cycle times shorter than at minimum power are not feasible due to increased dust emissions and no additional energetic benefit. Cycle times longer than at minimum power may lower the dust emissions at the cost of increased power consumption. Lowering filter face velocity can greatly lower the power consumption of baghouse filters, having implications on filter layout.

This is an open access article under the terms of the Creative Commons Attribution License, which permits use, distribution and reproduction in any medium, provided the original work is properly cited.

Supporting Information available online

Keywords: Energy optimization, Filtration, Particle emissions, Process efficiency, Pulse jet-cleaned filters

Received: February 03, 2023; *revised:* March 24, 2023; *accepted:* May 11, 2023

DOI: 10.1002/ceat.202300080

1 Introduction

Increasing process efficiency and minimizing the power consumption of industrial processes is one of many important measures to lower carbon dioxide emissions to lessen the impact of climate change and staying economically sustainable when facing rising energy costs. Pulse jet-cleaned filters have remained a key technology for dust separation in many industrial processes for several decades and have kept their relevance to this day [1]. The application spectrum for baghouse filters ranges from industrial processes (e.g., cement or aluminum production, food sector, wood processing [2–6]) to smaller-scale applications (e.g., incineration plants, dedusting systems for worker protection [7, 8]).

The operation of filters often follows a strict framework (e.g., Δp- or Δt-controlled criterion for filter regeneration)[1)] [9] and a re-evaluation of filter operation regarding energy aspects has the potential to improve process efficiency in the future [10]. While the research foundations for pulse jet-cleaned filters have been laid in the past by, e.g., Löffler [11] or Leith and Ellenbecker [12], present filter operation under demanding conditions still poses its individual challenges [13]. To list some examples, (nano-)particles can cause clogging of the filter material with particulate matter so that the differential pressure increases drastically and the filtration of a protective pre-coat prior to the nanoparticle aerosol might be necessary [7, 14, 15]. High temperatures and toxic gases push the limits of conventional (e.g., polyester needle-felt) filter media and rigid ceramic filter elements have to be used [16–18].

The operation of pulse jet-cleaned filters – while simple on first glance – offers room for highly flexible cleaning and operation strategies that impact particle emissions and the power consumption. During filter operation, particles are separated primarily on the surface of the filter medium, causing the formation of a dust cake with high separation efficiency and an increase in differential pressure. After a regeneration criterion is met (e.g., exceeding of a maximum differential pressure Δp_{max} or a cycle time Δt), a jet pulse from the clean gas side causes the rapid deformation of the filter element and subsequent cake detachment [9]. This leaves the filter medium prone to particle penetration for a short duration (hence causing an "emission peak") until a sufficient dust cake has been deposited on the surface of the medium [19].

The biggest contributors regarding power consumption of filter operation are the consumption of pressurized air P_{reg} for filter regeneration and the fan power P_{fan} caused by the differential pressure due to the flow through the filter medium and the filter cake [10, 20, 21]. Both of these contributions are

1) List of symbols at the end of the paper.

Peter Bächler https://orcid.org/0000-0001-9172-5880 (peter.baechler@kit.edu), Dr.-Ing. Jörg Meyer, Prof. Dr.-Ing. habil. Achim Dittler
Karlsruhe Institute of Technology, Institute of Mechanical Process Engineering and Mechanics, Strasse am Forum 8, 76131 Karlsruhe, Germany.

 © 2023 The Authors. Chemical Engineering & Technology published by Wiley-VCH GmbH

dependent on each other. Higher pulse intensities (e.g., tank pressures for filter regeneration p_{tank}) and shorter time durations between regenerations Δt_{cycle} may lead to a lower differential pressure through better and more frequent cake detachment, but in turn, the consumption of pressurized air rises. Increased tank pressures are known to lead to higher dust emissions as, e.g., seams of the filter element cannot clog sufficiently and remain a source for particle penetration, but may grant a lower residual differential pressure after regeneration due to improved cake detachment [19, 22–24].

Klein et al. [21] have shown the relevance of the efficiency of the nozzle geometries for the jet pulse and discussed the power consumption of pulse jet-cleaned filters. According to Klein et al., roughly 15 % of the required power is caused by the consumption of pressurized air. The remaining 85 % can be attributed to the differential pressure (roughly 11 % housing, 59 % filter cake, 8 % residual pressure drop of the filter medium, 7 % lateral flow through the bag) between raw-gas side and clean-gas side. While the investigation was based on a certain application scenario (filter face velocity: 1 m min^{-1}, length of the bag 6 m, and tank pressure for regeneration 6 bar) it serves as a general guideline [21].

In another study, Ho et al. determined an economically optimal cycle time of 10 s for pulse jet-cleaned filters (pleated filter) on an industrial scale [25]. Krammer et al. also performed investigations regarding an optimal cycle time for filter operation, whereby the optimization criterion was focused on differential pressure levels [26]. Caputo and Pelagagge examined the economic optimum for baghouse filters, identifying optimal filtration velocities for certain filtration times [27]. While the economic situation is market-dependent, an energy evaluation has the advantage of universal applicability even for fluctuating energy prices.

From an emissions perspective, modern (membrane) filter media may provide (almost) zero emission levels [28]. Mainly leaks of the filter medium or the plenum plate, small defects of the filter medium, or the seams of the filter element due to the manufacturing process can cause increased particle emissions [29–31]. In the context of the current draft of the Common Waste Gas Treatment in the Chemical Sector-Best Available Techniques Reference Document (WGC-BREF), a restriction of dust emissions for fabric filters of 5 mg m^{-3} (in case of dust mass flows > 0.05 kg h^{-1} at each stack with unique conditions at the outlet) is discussed [32]. In case of a bag failure or unfavorable operation conditions, these limits could potentially be exceeded. Conventional emission monitoring is performed at the outlet of the filter house, e.g., via gravimetrical measurement or triboelectric sensors or "filter guards" [33].

The identification of leaks can be performed, e.g., with the help of fluorescent dust for visual identification during a plant shutdown. Innovative sensor technology has been proposed by Li et al. in the form of an optical fiber sensor to identify damaged filter elements [34]. In previous publications, the suitability of the identification of leaks and spatial emission monitoring by application of scattered-light-based particulate matter (PM) sensors has been discussed in detail demonstrating the potential of improved emission monitoring in filtration applications [28, 35, 36].

This study, consisting of two individual articles, aims to combine the two most prominent performance indicators of filter operation, namely, the required power for filter operation and particle emissions, to enable a better evaluation of beneficial operation settings and favorable cycle times. In this first article, the operation of a small-scale baghouse filter is discussed under energy-related and particle emission-related criteria. The power consumption of the baghouse filter is calculated according to equations proposed by Höflinger and Laminger [2, 14] (compare Sect. 2.3). The second article will deal with the modeling of filter operation applying and expanding on the calculation basics introduced by Löffler [11]. Modeling has the potential to improve the layout of baghouse filters and check existing plants regarding energy-efficient operation as well as validating the experimental results.

2 Experimental Setup, Materials, Measurement Technology, and Experimental Methodology

2.1 Pilot Plant-Scale Baghouse Filter

The experiments have been performed in a small-scale baghouse filter (Fig. 1) with a total of nine filter bags (4.14 m^2 installed filter area).

A radial blower creates a circulating air flow through the testing facility. Dust is added at two separate points: new dust is added from a silo to enable a constant particle size distribution and already separated dust is recirculated to grant long-term economic operation. The raw-gas dust concentration is monitored via an extinction measurement before entering the filter house. The extinction measurement has been calibrated for several gravimetrical concentration levels (dispersion via screw-feeders with varying rotational speed). After entering the filter house, dust is separated from the air flow at the surface of the filter medium. Each filter bag can be regenerated individually (cleaning of approx. 1/9th of installed filter area for each regeneration). During the experiments, a time-controlled regeneration algorithm was selected so that a single filter bag is regenerated after a time interval Δt_{cycle} following a "bag-by-bag" cleaning pattern. The total particle emission penetrating the filter bags after regeneration is monitored employing a highly developed laboratory aerosol spectrometer (Promo® 2000 with welas® 2100 sensor) from the manufacturer Palas®.

Several different parameters have been adjusted and evaluated regarding their energy demand (respectively required power for filter operation) and particle emission. Tab. 1 gives an overview on the varied and constant process parameters.

2.2 Filter Medium and Test Dust

The employed filter medium was a polyester needle-felt with a singed upstream side. Specifications of the filter medium are summarized in Tab. 2. Prior to the experiments, the filter bags were aged up to 300 complete filtration cycles each so that particle emissions and residual pressure drop of the filter elements are stabilized and any consecutive filter aging effects are negligible compared to the variations performed in the parameter study [23]. The filter medium is representative for commonly

 © 2023 The Authors. Chemical Engineering & Technology published by Wiley-VCH GmbH

15214125, 0, Downloaded from https://onlinelibrary.wiley.com/doi/10.1002/ceat.202300080 by Cochrane Germany, Wiley Online Library on [08/06/2023]. See the Terms and Conditions (https://onlinelibrary.wiley.com/terms-and-conditions) on Wiley Online Library for rules of use; OA articles are governed by the applicable Creative Commons License

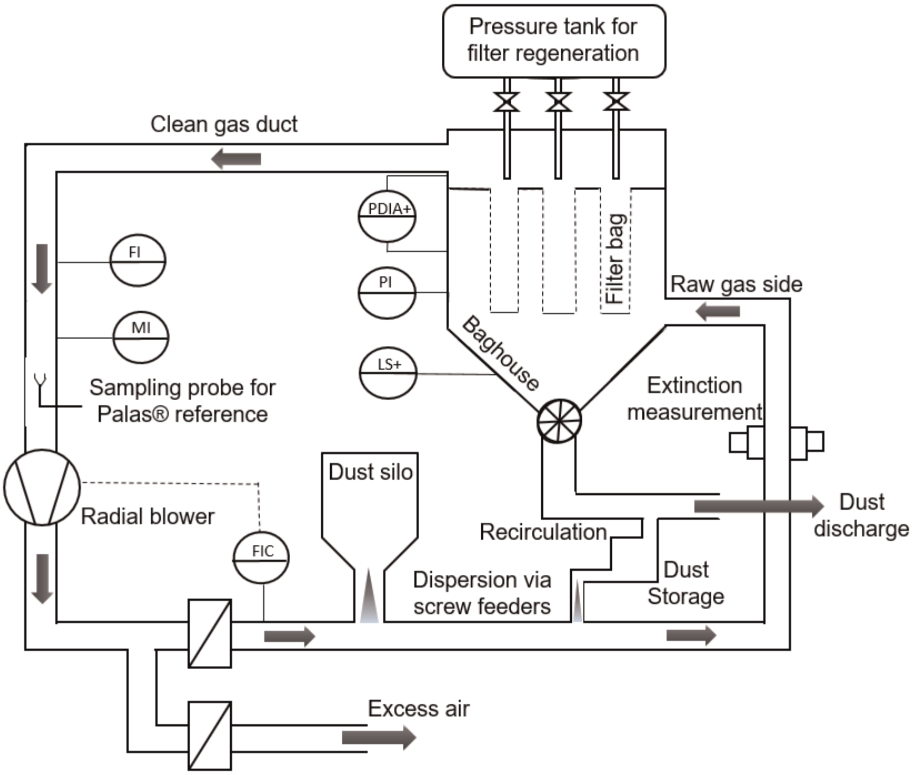

Figure 1. Schematic overview of the baghouse filter (operating parameters listed in Tab. 1) – image modified from [28].

Table 1. Varied and constant process parameters for the study.

Parameter	Value
Filter face velocity [$cm\,s^{-1}$]	2, 2.5, and 3.3
Raw-gas concentration $c_{raw\text{-}gas}$ [$g\,m^{-3}$]	15, 30, and 40
Tank pressure p_{tank} [bar]	3 and 6
Cleaning interval Δt_{cycle} [s]	10–180
Electrical valve opening time [ms]	150
Filter medium	Needle felt (compare Tab. 2)
Test dust	PURAL SB®

Table 2. Specifications of the needle-felt filter medium.

Parameter	Value
Area weight [$g\,m^{-2}$]	600
Thickness [mm]	2
Permeability (at 200 Pa) [$L\,dm^{-2}min^{-1}$]	70
Fiber material and remarks	PE, singed upstream side

used needle-felt filter media used in the industrial applications. The bags have a length of 125 cm and a diameter of 11.7 cm, what is on the lower end of typical bag geometries.

The test dust PURAL SB® is an alumina monohydrate powder from the manufacturer Sasol®. A more in-depth evaluation of the test dust, including the particle size distribution across a wider range (from 10 nm to 200 µm) measured by different instruments, can be found in a previous publication [37]. The test dust has a mass median diameter of approx. 35 µm as determined by laser diffraction. The dust is free-flowing and does not tend to agglomerate, causing a significant fine-dust fraction in the dispersed state. Thus, the dust tends to cause high emissions during filter tests.

Note that the reported data in this publication is only valid for this system of test dust and filter medium. Different dust properties and types of filter media, e.g., membrane filter media, may lead to different conclusions regarding optimal process parameters.

2.3 Methodology for the Evaluation of Filter Operation under Energy-Related and Particle Emission-Related Criteria

Höflinger et al. proposed a method to evaluate filter media based on energy criteria in a filter test rig based on DIN ISO 11057 [38]. They took into account the differential pressure across the filter medium as well as the consumption of pressurized air from the jet pulse by applying the following equation in order to calculate the total power consumption of filter operation P_{Filter} (equation modified from [10, 20]):

$$P_{Filter} = \dot{V}\Delta p_{Filter} + \frac{V_{Tank}\Delta p_{Tank}}{\Delta t_{cycle}} \quad (1)$$

where $\dot{V}$ is the volume flow through the filter, Δp_{Filter} is the differential pressure between raw-gas side and clean-gas side, V_{Tank} is the volume of the vessel containing the pressurized air, Δp_{Tank} is the pressure drop within the vessel caused by releasing the jet pulse for filter regeneration, and Δt_{cycle} the time interval between filter regenerations or cleaning frequency. The equation can be split into two separate parts, representing the required fan power due to the differential pressure across the

 © 2023 The Authors. Chemical Engineering & Technology published by Wiley-VCH GmbH

15214125, 0, Downloaded from https://onlinelibrary.wiley.com/doi/10.1002/ceat.202300080 by Cochrane Germany, Wiley Online Library on [08/06/2023]. See the Terms and Conditions (https://onlinelibrary.wiley.com/terms-and-conditions) on Wiley Online Library for rules of use; OA articles are governed by the applicable Creative Commons License

filter medium and the dust cake and the required average power consumption of the jet-pulse cleaning.

$$P_{\text{Filter}} = P_{\text{fan}} + P_{\text{reg}} \quad (2)$$

$$P_{\text{fan}} = \dot{V}\Delta p_{\text{Filter}} \quad (3)$$

$$P_{\text{reg}} = \frac{V_{\text{Tank}}\Delta p_{\text{Tank}}}{\Delta t_{\text{cycle}}} \quad (4)$$

The equation itself can be transferred and used aside from filter testing to estimate the required energy demand for baghouse filters. The underlying experimental procedure was presented at the Filtech 2023 conference [39]. To evaluate filter operation based on the energy consumption, the determination of an average differential pressure Δp_{Filter} is necessary for a certain set of parameters. The pressure drop during the jet pulse Δp_{Tank} has to be determined for individual tank pressures and valve opening times (constant valve opening time of 150 ms in this study).

The cycle time has been adjusted during each experimental run for each parameter, ranging from a maximum cycle time (e.g., 180 s) down to 10 s (longest possible sequence: 180 s → 150 s → 120 s → 90 s → 60 s → 45 s → 30 s → 20 s → 10 s) to create several differential pressure levels. Note that longer cycle times above 90 s are at the upper limit of the capacity of the radial blower of the testing facility for the highest adjusted filter face velocity of 3.3 cm s^{-1} and the volume flow may decrease by approx. 10 % during the cycle. Therefore, the starting point of the sequence was adjusted dependent on the corresponding parameters, ensuring that an energetic optimum could be identified for each setting.

The exact cycle times within the sequence (after selecting an initial starting cycle time) were kept constant for each experiment and set of parameters, starting at the highest cycle time ranging down to the lowest cycle time of 10 s. The average differential pressure and the average particle emission were determined from the experimental data at the end of the corresponding cycle time setting to gain a representative value.

For the determination of an average power consumption of the pressurized air for filter regeneration, the pressure drop Δp_{Tank} was determined in a preliminary experiment for multiple tank pressures. The volume of the tank V_{Tank} is 0.011 m^3 so that the calculation of the energy consumption for filter regeneration P_{reg} is possible. More information regarding the experimental procedure can be found in the Supporting Information.

Fig. 2 displays a summary of the determination of a characteristic operation curve for filter operation by combining the total required power for filter operation (consisting of P_{fan} and P_{reg}) and the particle emission. $PM_{2.5}$ concentrations were selected as benchmark values for the particle emission, as the fine dust fraction is of significant importance regarding human health and was also presented in older studies when measuring the emission with scattered-light based low-cost PM sensors [28, 35, 36]. $PM_{2.5}$ represents the fine dust fraction of the emission (classification of particles following a separation curve with a cut size of 2.5 µm). Plotting the total energy consumption versus the particle emission yields the operation curve.

The operation curve enables the identification of favorable operation regions at (or close to) the minimum power. A more detailed guideline on how to read the operation curve can be found in the Supplementary Information. In general, operation points on the right side of the power minimum (red line – higher energy consumption and higher emissions) are unfavorable. To the left of the power minimum (green line), emissions are lower at the cost of a certain increase of fan power, as the contribution of pressurized air consumption becomes (almost) negligible. Exceeding feasible cycle times may yield an increasingly high total power consumption that outweighs the lower dust emission due to less frequent regenerations. Note that the low spectrum of employed cycle times (e.g., 10 and 20 s) borders unstable operation (almost constant regeneration of a large fraction of installed filter area and no cake formation) and thus, is not praxis-relevant [40].

The results of the study are within reasonable agreement with the publication by Klein et al. [21], where approximately 15 % of the total power can be allocated to filter regeneration and the remaining 85 % can be attributed to the differential pressure across housing and filter. The contributions of fan power and filter regeneration to the total power at the corre-

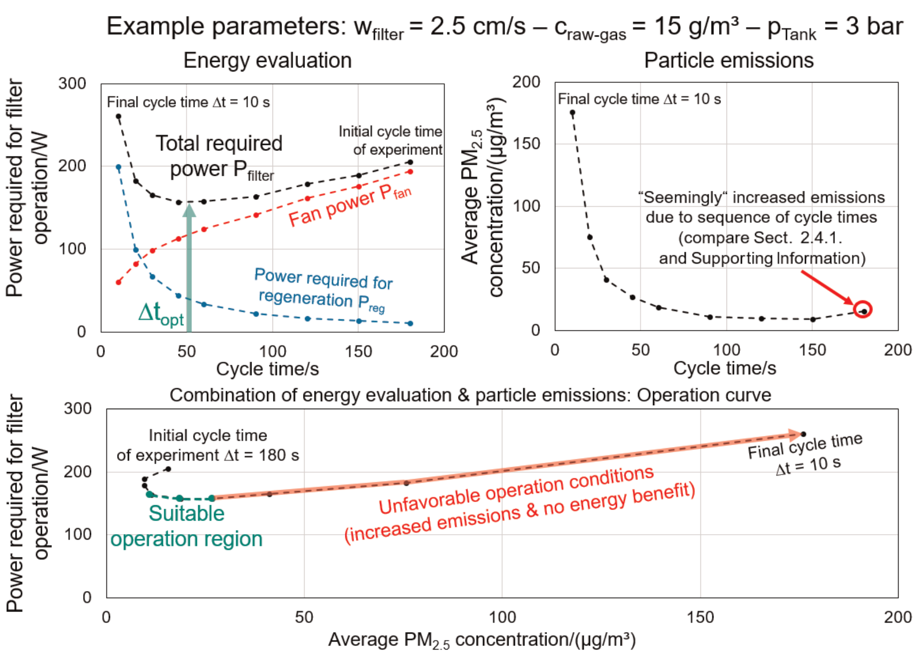

Figure 2. Evaluation of filter operation based on power consumption and particle emissions for a certain set of parameters (w_{filter} = 2.5 cm s^{-1}, $c_{\text{raw-gas}}$ = 15 g m^{-3}, p_{Tank} = 3 bar).

 © 2023 The Authors. Chemical Engineering & Technology published by Wiley-VCH GmbH

15214125, 0, Downloaded from https://onlinelibrary.wiley.com/doi/10.1002/ceat.202300080 by Cochrane Germany, Wiley Online Library on [08/06/2023]. See the Terms and Conditions (https://onlinelibrary.wiley.com/terms-and-conditions) on Wiley Online Library for rules of use; OA articles are governed by the applicable Creative Commons License

sponding minimum are ranging between 60–80 % fan power and 40–20 % filter regeneration for the experiments. Note that the determined fan power does not include fan efficiencies or electrical efficiencies, so that the actual contribution would be somewhat higher and a little closer to the data reported by Klein et al.

3 Results and Discussion

3.1 Variation of Raw-Gas Concentration

Different cycle time settings were adjusted at a constant tank pressure for filter regeneration of 3 bar and a filter face velocity of 2 cm s^{-1} at varying raw-gas concentration levels. The operation curves of the experiments were derived according to Sect. 2.3 and are displayed in Fig. 3.

A shift towards higher power requirements occurs with an increase in raw-gas concentration (global trend of operation curves) due to thicker dust cakes. Adjusting the cycle times cannot offset the increment in differential pressure due to the increased dust load on the filter bags. The region close to the power minimum is of actual interest regarding viable settings for filter operation. The power minimum for lower raw-gas concentrations is located at a lower overall power consumption combined with longer cycle times so that filter regeneration is required less frequently. From an emissions perspective, all operation curves are in a similar region ($PM_{2.5}$ emission lower than 30 µg m^{-3} at the optimum). Particle emissions are lower for the shorter cycle times, mainly 10 and 20 s, at higher raw-gas concentrations. Increased dust load causes the rapid formation of a dust cake even for the shorter cycle times what may seem beneficial at first, however, the shorter cycle times of 10 and 20 s are far outside an energetically suitable operation region.

Fig. 4 shows the potential benefit of incorporating energy criteria into the evaluation of filter operation via a detail view of the region around the power minimum.

At the region close to the power minimum, small adjustments regarding the cycle time Δt_{cycle} may significantly impact particle emissions and power consumption. In the figure, the green lines represent a favorable increase in cycle time, where emissions can be lowered significantly at almost no increase in total power. Purple lines indicate a reasonable decrease in particle emission when compared to the additional power requirement. Red lines display unfavorable shifts in cycle times with significantly increased power consumptions with negligible impact on particle emissions.

As an example, the energetic optimum at 15 g m^{-3} raw-gas concentration can be identified at 90–60 s, where there is no

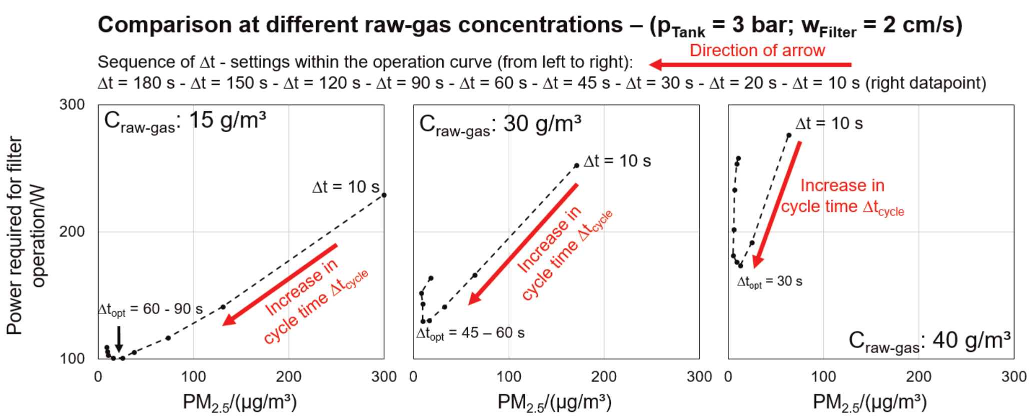

Figure 3. Operation curve of filter operation at different raw-gas concentrations (w_{filter} = 2 cm s^{-1}, p_{Tank} = 3 bar).

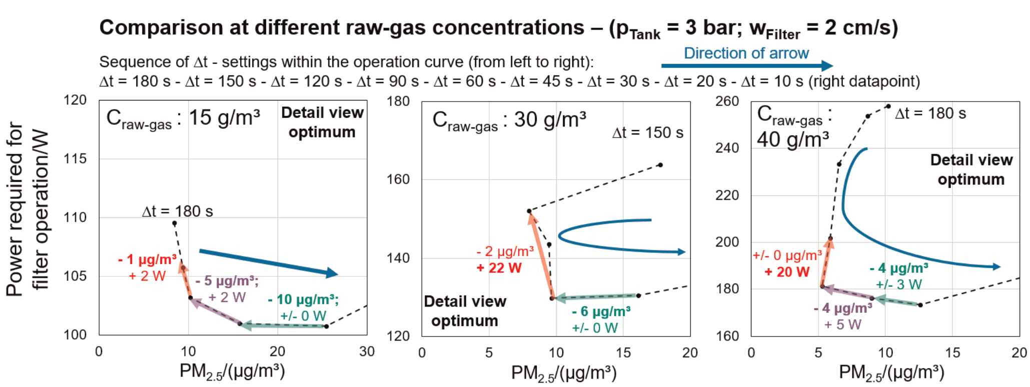

Figure 4. Detail view of the power minimum of the operation curves at different raw-gas concentrations (w_{filter} = 2 cm s^{-1}, p_{Tank} = 3 bar).

 © 2023 The Authors. Chemical Engineering & Technology published by Wiley-VCH GmbH

15214125, 0, Downloaded from https://onlinelibrary.wiley.com/doi/10.1002/ceat.202300080 by Cochrane Germany, Wiley Online Library on [08/06/2023]. See the Terms and Conditions (https://onlinelibrary.wiley.com/terms-and-conditions) on Wiley Online Library for rules of use; OA articles are governed by the applicable Creative Commons License

significant difference between the total power at both cycle times. Thus, the longer cycle time of 90 s is overall preferable, due to less frequent regenerations and lower particle emissions. In order to further lower particle emissions, the cycle time could be increased further to 120 s. While the energetic investment is moderate, if not negligible, the decrease in particle emission is significant. A further increase from 120 s to 150 s is not sensible, as the energetic investment increases further but the impact on dust emissions is rather low compared to the previous step from 90 s to 120 s).

Summarizing, an increase in raw-gas concentration shifts the power minimum towards higher overall power consumption at a shorter cycle time, making more frequent regenerations more feasible. At the corresponding filter face velocity of 2 cm s^{-1}, the cycle times were sufficiently long in order to not suffer exceedingly high dust emissions.

3.2 Variation of Filter Face Velocity

After the variation of raw-gas concentration, the filter face velocity has been varied for two distinct levels of raw-gas concentration (15 and 30 g m^{-3}). Since the filter face velocity is defined as the total volume flow divided by the available filter area, adjusting the filter face velocity in the baghouse filter is only possible by changing the volume flow (constant installed filter area). Due to the direct correlation between flow velocity and pressure drop, the required power has been related to the total volume flow in Fig. 5 to grant directly comparable conditions (specific energy demand in Wh m^{-3}).

The results at the corresponding filter face velocities are qualitatively similar to the previous chapter at 2 cm s^{-1} filter face velocity. At the higher raw-gas concentration, the operation curve is shifted towards higher power consumptions and the power minimum is shifted towards shorter cycle times (more frequent regeneration). The results are in line with the investigations of Saleem et al. where increased filter face velocities led to shorter cycle times and a higher specific cake resistance for a Δp-controlled filter operation [41]. The particle emission in the relevant operation region (cycle times equal to or larger than the cycle time at the minimum) are at a low level with (almost) negligible differences regarding the varied parameters.

A lower filter face velocity is highly beneficial from an energy point of view. Lowering the filter face velocity would potentially allow for higher raw-gas concentrations (similar level of operation curves at 30 g m^{-3} and lower filter face velocity compared to 15 g m^{-3} and the next-higher filter face velocity). Longer cycle times are also beneficial from a wear and materials perspective, as less frequent regenerations can prolong the lifetime of filter elements. A summary of the power consumptions at the minimum with the corresponding cycle time can be found in Sect. 3.3 in Fig. 6.

Following the energy evaluation, economic aspects would have to be taken into account. The findings give major implications to the layout of filter houses regarding the required filter area. Facing rising energy costs, installing a larger amount of filter area to keep the filter face velocity as low as possible compared to the typical layout guidelines, e.g., stated in VDI3677 [42], might be feasible. However, additional filter area of course also causes additional investment and maintenance costs when replacing filter elements. Increasing the filter area is in most cases retroactively not possible for existing filter houses and the volume flow of an industrial facility is (in most cases) fixed and cannot be varied. Some industrial filters operate under a fan with constant rotary speed. Here, it might be beneficial to lower the rotary speed to save energy, if process stability is not in danger.

3.3 Variation of Tank Pressure for Filter Regeneration

The experiments presented in Sect. 3.2 were repeated at a higher tank pressure for filter regeneration (6 bar compared to 3 bar) to demonstrate the effect on particle emissions and total power of raising the regeneration intensity.

The power minimum of the corresponding experimental parameters is summarized in Fig. 6. When increasing the tank

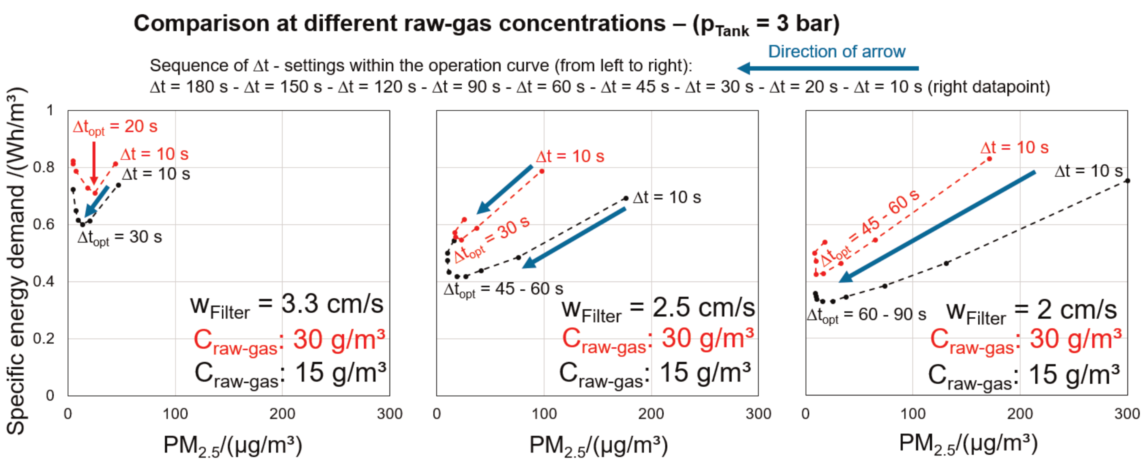

Figure 5. Operation curve of filter operation at different raw-gas concentrations (15 and 30 g m^{-3}) and filter face velocities (2, 2.5, 3.3 cm s^{-1}).

 © 2023 The Authors. Chemical Engineering & Technology published by Wiley-VCH GmbH

15214125, 0, Downloaded from https://onlinelibrary.wiley.com/doi/10.1002/ceat.202300080 by Cochrane Germany, Wiley Online Library on [08/06/2023]. See the Terms and Conditions (https://onlinelibrary.wiley.com/terms-and-conditions) on Wiley Online Library for rules of use; OA articles are governed by the applicable Creative Commons License

These are not the final page numbers! ↘↘

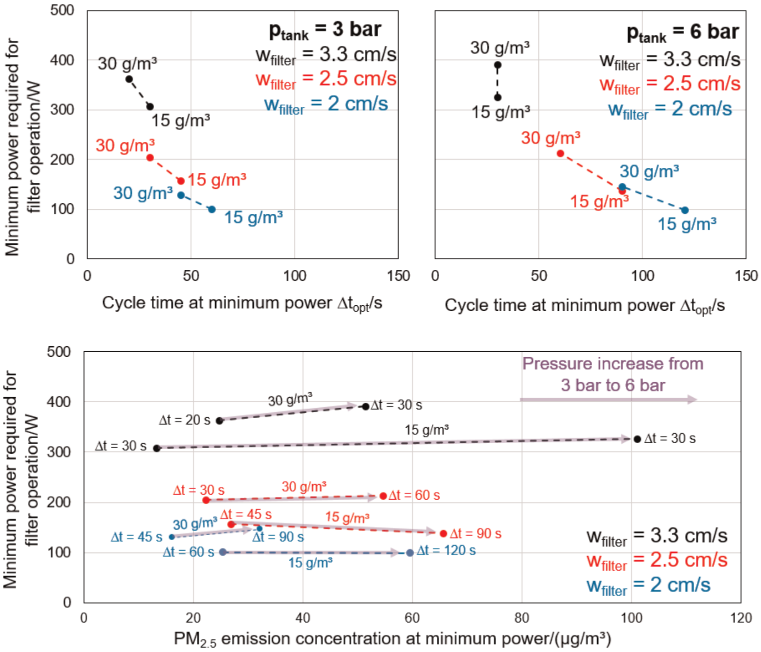

Figure 6. Comparison of cycle times at minimum power regarding energy demand and particle emissions for two different tank pressures (3 and 6 bar) at varying raw-gas concentrations and filter face velocities. In case of a less pronounced power minimum (multiple datapoints), only a single datapoint is displayed (compare Figs. 3 and 5).

pressure, the power requirement due to the jet pulse/filter regeneration rises according to Eq. (4), as the pressure drop Δp_{tank} within the pressure vessel becomes higher.

The bottom image in Fig. 6 clearly demonstrates the potential emission problems of raising the tank pressure. Despite the longer cycle times at the power minimum for the 6-bar measurements, the particle emission increases by approx. a factor of 2. There is almost no benefit of raising the tank pressure from an energy point of view, as the differences in total power between the individual settings are almost negligible. The cycle times of the 6 bar tank pressure are approximately higher by a factor of 2 for the filter face velocities of 2.5 and 2 cm s^{-1}. Less frequent regenerations are, in theory, beneficial from a wear and materials perspective. However, the higher pulse intensity also increases the wear on the filter element, so that there is no obvious benefit. According to the results of Tsai et al. [22], increasing the tank pressure above certain limits does not significantly lower the residual pressure difference after regeneration. There may be more beneficial pulse intensities from an energy perspective. Additional data for 4.5 bar tank pressure and a raw-gas concentration of 30 g m^{-3} is reported in the Supporting Information.

Summarizing, increasing the tank pressure for filter regeneration overall lowered the contribution of the required fan power (lower differential pressure level) due to a more thorough cleaning of the filter element and lower residual pressures after filter regeneration. The additional energetic investment due to increased pressures mitigated the benefit of a lower differential pressure level. While higher tank pressures shifted the energetic optimum to higher cycle times, the particle emissions were greatly increased due to the higher pulse intensity so that raising the tank pressure above certain limits is never recommended outside certain scenarios, e.g., regeneration issues or conglutination of filter elements.

4 Summary and Outlook

The operation of a pulse jet-cleaned filter was evaluated in a pilot-scale baghouse filter taking into account power consumption and particle emission. The power required for filter operation was determined according to the equations proposed by Höflinger et al., considering the fan power (product of volume flow and average differential pressure for a set of parameters) and an average power representing the consumption of pressurized air for jet-pulse cleaning. Particle emissions were measured using an optical aerosol spectrometer.

Several different parameters were varied. The main results of the parameter study are summarized in Tab. 3. Note that the results are based on investigations using a single type of filter medium (needle-felt) and test dust (free-flowing/non-agglomerating). Different dust properties and filter media may lead to different conclusions; however, the qualitative observations should be valid for many applications.

Higher raw-gas concentrations and higher filter face velocities led to qualitatively similar results in the form of an increase of the total power consumption due to higher differential pressure levels and a decrease in the cycle time at minimum power (more frequent regenerations). The differences in particle emission were negligible at feasible operation regions and sufficiently long cycle times. Raising the tank pressure did not offer energetic benefits, as the lower power requirement due to lower differential pressure levels got mitigated by increased power consumption of the higher intensity pressure pulse.

Table 3. Summary of the results of the parameter variation.

Parameter variation increase of:	Total power consumption	Cycle time at the power minimum	Particle emission
Raw-gas concentration	Increase	Decrease More frequent regeneration	Constant at relevant operation region
Filter face velocity	Increase	Decrease More frequent regeneration	Constant at relevant operation region
Tank pressure	(Almost) constant	Increase Less frequent regeneration	Increase

 © 2023 The Authors. Chemical Engineering & Technology published by Wiley-VCH GmbH

15214125, 0, Downloaded from https://onlinelibrary.wiley.com/doi/10.1002/ceat.202300080 by Cochrane Germany, Wiley Online Library on [08/06/2023]. See the Terms and Conditions (https://onlinelibrary.wiley.com/terms-and-conditions) on Wiley Online Library for rules of use; OA articles are governed by the applicable Creative Commons License

The results demonstrate the importance of taking into account energy criteria when evaluating filter operation. While many results may seem evident (e.g., an increase in raw-dust concentration requires a decrease in cycle time in order to remain at a feasible differential pressure level), the exact quantification of energetically beneficial operation points can put current operation strategies into question and offer a perspective on optimization potential.

Many industrial filters follow more or less strict operation frameworks. Incorporating these results into operation strategies, e.g., monitoring raw-gas concentrations, and dynamically adjusting the cycle time towards favorable conditions may improve the energy efficiency of pulse jet-cleaned filters.

In part 2 of this study, the experimental results of this article will be implemented in modeling of filter operation applying and enhancing the calculation basics by Löffler [11]. This has the potential to give layout advice regarding filter operation and help plant operators predict and optimize the energy demand of their filter when changing existing parameters.

Supporting Information

Supporting Information for this article can be found under DOI: https://doi.org/10.1002/ceat.202300080.

Acknowledgment

The authors acknowledge the financial support and close cooperation of Filterkonsortium at KIT. Filterkonsortium at KIT unites leading companies in the fields of fiber and media production, assembly, plant engineering, and measurement technology with the research activities of the research group Gas-Particle-Systems of the Institute of Mechanical Process Engineering and Mechanics (MVM). The members of Filterkonsortium at KIT are as follows: BWF Tec GmbH & Co. KG, ESTA Apparatebau GmbH & Co. KG, Evonik Fibres GmbH, Freudenberg Filtration Technologies SE & Co. KG, Junker-Filter GmbH, MANN+HUMMEL GmbH, PALAS GmbH, Sick AG. We acknowledge that part of the materials (Sect. 2.3) and parts of the Supporting Information have been first presented at FILTECH 2023. Open access funding enabled and organized by Projekt DEAL.

The authors have declared no conflict of interest.

Symbols used

$c_{\text{raw-gas}}$	[g m^{-3}]	raw-gas dust concentration
Δp	[Pa]	differential pressure
Δp_{filter}	[Pa]	differential pressure between raw-gas side and clean gas side across the filter medium (including the dust cake)
Δp_{tank}	[bar]	pressure drop in the pressure vessel supplying the pressurized air for the jet pulse
P_{fan}	[W]	fan power
P_{filter}	[W]	total energy consumption of filter operation
$PM_{2.5}$	[μg m^{-3}]	fine dust fraction of the emission (classification of particles following a separation curve with a cut size of 2.5 μm)
P_{reg}	[W]	energy consumption due to filter regeneration/consumption of pressurized air
$\Delta t/\Delta t_{\text{cycle}}$	[s]	time interval between regenerations of each individual filter element (if each of the nine filter elements was regenerated, it is referred to as a "complete filtration cycle")
Δt_{opt}	[s]	cycle time at the power minimum of an operation curve
$\dot{V}$	[m^3 h^{-1}]	volume flow
V_{tank}	[m^3]	volume of the pressure vessel supplying the pressurized air for the jet pulse
w_{filter}	[cm s^{-1}]	filter face velocity

References

[1] W. Peukert, A. Bück, *Chem. Ing. Tech.* **2022**, *95 (1–2)*, 19–25. DOI: https://doi.org/10.1002/cite.202200159

[2] X.-L. Huang, A. M. El Badawy, M. Arambewela, R. Adkins, T. Tolaymat, *Chemosphere* **2015**, *134*, 25–30. DOI: https://doi.org/10.1016/j.chemosphere.2015.03.033

[3] J. O. Litchwark, J. Winchester, J. J. Nijdam, *Powder Technol.* **2015**, *284*, 379–386. DOI: https://doi.org/10.1016/j.powtec.2015.06.056

[4] J. Wilanowicz, W. Grabowski, M. Andrzejczak, A. Chromiec, *Procedia Eng.* **2013**, *57*, 1269–1277. DOI: https://doi.org/10.1016/j.proeng.2013.04.160

[5] X. Simon, D. Bémer, S. Chazelet, D. Thomas, *Powder Technol.* **2014**, *261*, 61–70. DOI: https://doi.org/10.1016/j.powtec.2014.04.028

[6] M. G. Cora, Y.-T. Hung, *Environ. Qual. Manage.* **2002**, *11 (4)*, 53–64. DOI: https://doi.org/10.1002/tqem.10041

[7] S. Schiller, H. J. Schmid, *Powder Technol.* **2015**, *279*, 96–105. DOI: https://doi.org/10.1016/j.powtec.2015.03.048

[8] F. Schott, G. Baumbach, D. Straub, H. Thorwarth, U. Vogt, *Biomass Bioenergy* **2022**, *163*, 106520. DOI: https://doi.org/10.1016/j.biombioe.2022.106520

[9] K. T. Hindy, *Atmos. Environ.* **1986**, *20 (8)*, 1517–1521. DOI: https://doi.org/10.1016/0004-6981(86)90240-4

[10] W. Höflinger, T. Laminger, *Energy Sustainability* **2013**, *4*, 145–155. DOI: https://doi.org/10.2495/ESUS130121

[11] F. Löffler, *Staubabscheiden*, Georg Thieme, Stuttgart **1988**.

[12] D. Leith, M. J. Ellenbecker, *Aerosol Sci. Technol.* **1982**, *1 (4)*, 401–408. DOI: https://doi.org/10.1080/02786828208958604

[13] W. Peukert, C. Wadenpohl, *Powder Technol.* **2001**, *118 (1–2)*, 136–148. DOI: https://doi.org/10.1016/S0032-5910(01)00304-7

[14] N. Khirouni, A. Charvet, D. Thomas, D. Bémer, *Process. Saf. Environ.* **2020**, *138*, 1–8. DOI: https://doi.org/10.1016/j.psep.2020.02.040

[15] E. H. Tanabe, P. M. Barros, K. B. Rodrigues, M. L. Aguiar, *Sep. Purif. Technol.* **2011**, *80 (2)*, 187–195. DOI: https://doi.org/10.1016/j.seppur.2011.04.031

 © 2023 The Authors. Chemical Engineering & Technology published by Wiley-VCH GmbH

15214125, 0, Downloaded from https://onlinelibrary.wiley.com/doi/10.1002/ceat.202300080 by Cochrane Germany, Wiley Online Library on [08/06/2023]. See the Terms and Conditions (https://onlinelibrary.wiley.com/terms-and-conditions) on Wiley Online Library for rules of use; OA articles are governed by the applicable Creative Commons License

[16] A. Dittler, H. F. Umhauer, *Powder Technol.* **2001**, *120 (3)*, 223–231. DOI: https://doi.org/10.1016/S0032-5910(01)00280-7
[17] G. Ahmadi, D. H. Smith, *Aerosol Sci. Technol.* **2002**, *36 (6)*, 665–677. DOI: https://doi.org/10.1080/02786820290038357
[18] J.-H. Kim, Y.-C. Kim, J.-H. Choi, *Korean J. Chem. Eng.* **2016**, *33*, 726–734. DOI: https://doi.org/10.1007/s11814-015-0211-y
[19] J. Binnig, J. Meyer, G. Kasper, *Powder Technol.* **2009**, *189 (1)*, 108–114. DOI: https://doi.org/10.1016/j.powtec.2008.06.012
[20] W. Höflinger, T. Laminger, *J. Taiwan Inst. Chem. Eng.* **2019**, *94*, 53–61. DOI: https://doi.org/10.1016/j.jtice.2017.07.035
[21] G.-M. Klein, T. Schrooten, T. Neuhaus, R. Kräbs, *Gefahrstoffe – Reinhalt. Luft* **2009**, *5*, 20633.
[22] C.-J. Tsai, M.-L. Tsai, H.-C. Lu, *Aerosol Sci. Technol.* **2000**, *35 (2)*, 211–226. DOI: https://doi.org/10.1081/SS-100100152
[23] O. Kurtz, J. Meyer, G. Kasper, *Chem. Eng. Technol.* **2016**, *39 (3)*, 435–443. DOI: https://doi.org/10.1002/ceat.201500340
[24] C. R. de Lacerda, P. Bächler, A. D. Schwarz, R. Sartim, M. L. Aguiar, A. Dittler, *Chem. Eng. Technol.* **2022**, *45 (7)*, 1354–1362. DOI: https://doi.org/10.1002/ceat.202200132
[25] C.-L. Ho, Y.-C. Tang, W.-C. Chiu, *Appl. Sci.* **2021**, *11 (22)*, 10941. DOI: https://doi.org/10.3390/app112210941
[26] G. Krammer, A. Kavouras, A. Anzel, *Chem. Eng. Technol.* **2003**, *26 (9)*, 951–955. DOI: https://doi.org/10.1002/ceat.200303032
[27] A. C. Caputo, P. M. Pelagagge, *Environ. Prog.* **2000**, *19 (4)*, 238–245. DOI: https://doi.org/10.1002/ep.670190410
[28] P. Bächler, J. Szabadi, J. Meyer, A. Dittler, *J. Aerosol Sci.* **2022**, *150*, 105644. DOI: https://doi.org/10.1016/j.jaerosci.2020.105644
[29] B. Bach, E. Schmidt, *J. Hazard. Mater.* **2007**, *144 (3)*, 673–676. DOI: https://doi.org/10.1016/j.jhazmat.2007.01.093
[30] O. Kurtz, J. Meyer, G. Kasper, *Particuology* **2017**, *30*, 40–52. DOI: https://doi.org/10.1016/j.partic.2016.08.001
[31] J. Li, Q. Wu, Y. Huang, J. Li, D. Wu, *Process. Saf. Environ.* **2022**, *158*, 282–290. DOI: https://doi.org/10.1016/j.psep.2021.12.012
[32] K. Daginnus, T. Marty, N. V. Trotta, T. Brinkmann, A. Whitfield, S. Roudier, *Best Available Techniques (BAT) Reference Document for Common Waste Gas Management and Treatment Systems in the Chemical Sector: Industrial Emissions Directive 2010/75/EU (Integrated Pollution Prevention and Control)*, JRC131915, European Union, Luxembourg **2023**. https://data.europa.eu/doi/10.2760/220326
[33] G. Wiegleb, *Gasmesstechnik in Theorie und Praxis*, Springer, Wiesbaden **2016**. DOI: https://doi.org/10.1007/978-3-658-10687-4
[34] J. Li, X. Lu, W. F. Wang, *Opt. Fiber Technol.* **2020**, *57*, 102218. DOI: https://doi.org/10.1016/j.yofte.2020.102218
[35] P. Bächler, V. Löschner, J. Meyer, A. Dittler, *Process. Saf. Environ.* **2022**, *160*, 411–423. DOI: https://doi.org/10.1016/j.psep.2022.02.005
[36] P. Bächler, J. Meyer, A. Dittler, *Chem. Ing. Tech.* **2023**, *95 (1–2)*, 178–188. DOI: https://doi.org/10.1002/cite.202200116
[37] P. Bächler, J. Meyer, A. Dittler, *Aerosol Sci. Technol.* **2022**, *56*, 394–402. DOI: https://doi.org/10.1080/02786826.2022.2027335
[38] DIN ISO 11057, *Air Quality – Test Method for Filtration Characterization of Cleanable Filter Media*, Beuth, Berlin **2016**.
[39] P. Bächler, J. Meyer, A. Dittler, On the trade-off between energy efficiency and particle emissions for pulse jet-cleaned filters, *Filtech 2023*, Cologne, February **2023**.
[40] H. Leubner, U. Riebel, *Chem. Ing. Tech.* **2003**, *75 (1–2)*, 82–86. DOI: https://doi.org/10.1002/cite.200390027
[41] M. Saleem, G. Krammer, R. U. Khan, M. S. Tahir, *Powder Technol.* **2012**, *224*, 28–35. DOI: https://doi.org/10.1016/j.powtec.2012.02.016
[42] VDI 3677 Blatt 1, *Filtering Separators – Surface Filters*, Beuth, Berlin **2010**.

 © 2023 The Authors. Chemical Engineering & Technology published by Wiley-VCH GmbH

15214125, 0, Downloaded from https://onlinelibrary.wiley.com/doi/10.1002/ceat.202300080 by Cochrane Germany, Wiley Online Library on [08/06/2023]. See the Terms and Conditions (https://onlinelibrary.wiley.com/terms-and-conditions) on Wiley Online Library for rules of use; OA articles are governed by the applicable Creative Commons License

Research Article: The operation of a pulse jet-cleaned filter is evaluated in a pilot-scale baghouse filter taking into account power consumption and particle emission. Suitable operation regions are identified and the trade-off between saving emissions and saving energy is discussed. Incorporating the results into operation strategies and dynamically adjusting the cycle time may improve the energy efficiency of such filters.

Operating Behavior of Pulse Jet-Cleaned Filters Regarding Energy Demand and Particle Emissions – Part 1: Experimental Parameter Study

Peter Bächler*, Jörg Meyer, Achim Dittler

Chem. Eng. Technol. **2023**, *46 (XX)*, XXX ... XXX

DOI: 10.1002/ceat.202300080

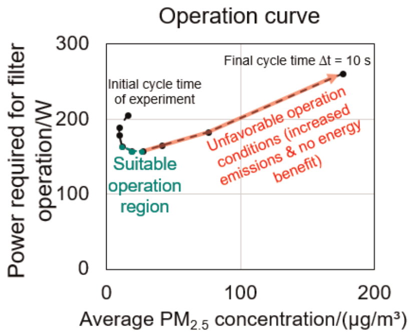

Supporting Information available online

 © 2023 The Authors. Chemical Engineering & Technology published by Wiley-VCH GmbH

15214125, 0, Downloaded from https://onlinelibrary.wiley.com/doi/10.1002/ceat.202300080 by Cochrane Germany, Wiley Online Library on [08/06/2023]. See the Terms and Conditions (https://onlinelibrary.wiley.com/terms-and-conditions) on Wiley Online Library for rules of use; OA articles are governed by the applicable Creative Commons License